

Received August 2, 2018, accepted September 10, 2018, date of publication October 9, 2018, date of current version December 19, 2018.

Digital Object Identifier 10.1109/ACCESS.2018.2874624

# Influence of High Voltage DC Transmission on Measuring Accuracy of Current Transformers

SHIHAI YANG<sup>1,2</sup>, GAN ZHOU<sup>3</sup>, (Member, IEEE), AND ZHINONG WEI<sup>1</sup>

<sup>1</sup>College of Energy and Electrical Engineering, Hohai University, Nanjing 210098, China

<sup>2</sup>Electric Power Research Institute, Jiangsu Electric Power Company, Nanjing 210019, China

<sup>3</sup>School of Electrical Engineering, Southeast University, Nanjing 210096, China

Corresponding author: Shihai Yang (ysh.young@163.com)

This work was supported in part by the Jiangsu Province Natural Science Fund under Grant BK20151412 and in part by the Science and Technology Foundation of State Grid Corporation of China under Grant 5210EF17001M.

**ABSTRACT** When the high-voltage direct current (HVDC) transmission is running under the monopole-ground-circuit operation mode, slight dc will be coupled into the nearby alternating current (ac) power grids and so has some negative influences, called dc bias phenomenon, on current transformers (CT). In this paper, based on the Preisach magnetization theory, a digital simulation method of CT is established, and then, its correctness has been verified by error calibration experiments. After that, the inherent mechanism of dc bias phenomenon is analyzed and concluded by simulating the coupling relationships among the magnetic flux density of iron core, exciting current, and coupling dc. Most importantly, we have built a coupling dc monitoring network for Jingpin to the south of Jiangsu (J2SJ) HVDC Project in China's Jiangsu Province, and based on the monitoring data and analysis results of CT's error varying with coupling dc, the actual influence of J2SJ HVDC on CT measuring accuracy is evaluated quantitatively.

**INDEX TERMS** Coupling DC, current transformer, DC bias, HVDC transmission, measuring accuracy.

## I. INTRODUCTION

When applied to long-distance, large-capacity power transmission, high voltage direct current (HVDC) transmission has significant technical advantages, such as its high stability, high reliability and unique ability of interconnecting different non-synchronous alternating current (AC) power grids [1]–[3]. With the implementation of energy policy “West to East Electricity Transmission”, HVDC transmission has achieved rapid development in China. By the end of 2014, China has built 18 HVDC projects whose total transmission capacity has ranked the first in the world. However, the operation of direct current (DC) power grid may have negative effects on AC power grid [4]–[9]. For instance, when the HVDC system is in a monopole overhaul status or a monopole fault happens, it will be running temporarily under the monopole-ground circuit (MGC) operation mode, in which a small quantity of direct current maybe couples into nearby AC power grid through the circuit which consists of the earth, neutral-point ground wires of main transformer (MT), primary windings of MT and current transformer (CT), and AC transmission lines. The aforementioned coupling DC will cause the abnormal bias of magnetic flux density in the iron core of MT or CT, called DC bias phenomenon, and

therefore the running performance of MT or CT will deviate obviously from its original design value.

This paper focuses on the influence of HVDC coupling current on CT's measuring accuracy. The two commonly used methods, formula derivation method and error calibration method, can only be used to assess quantitatively the influence of coupling DC, but they cannot give an insight into the principle of DC bias phenomenon [10], [11]. Therefore, based on Preisach magnetization theory, a digital simulation method of CT is established and its correctness has been verified by error calibration experiments. Then, the inherent mechanism of DC bias phenomenon is revealed by the simulation of coupling relationships among the magnetic flux density of iron core, exciting current and coupling DC, which is one important contribution of this paper. Most importantly, a coupling DC monitoring network for Jingpin to South of Jiangsu (J2SJ) HVDC project has been built in China's Jiangsu Province, and then based on the monitoring data and analysis results of CT's error varying with coupling DC, the actual influence of J2SJ HVDC on CT's measuring accuracy is evaluated quantitatively.

This paper is extended from our one-page conference digest [12]. This paper presents more detailed analysis about

the generation principle of coupling DC and its influence on CT, and develops a novel error calibration system for CT in DC bias condition compared with [12]. This paper is organized as follows. Section II explains the generation principle of HVDC coupling DC and analyzes the statistics data of occurrence frequency and duration time of HVDC coupling DC. Section III proposes a digital simulation method of CT and verified its correctness by error calibration experiments. Section IV reveals the inherent mechanism of DC bias phenomenon by simulation method proposed in Section III. Based on the actual monitoring data of coupling DC, Section V evaluates quantitatively the influence of J2SJ HVDC on CT's measuring accuracy.

### II. GENERATION PRINCIPLE OF COUPLING DC

This section explains the generation principle of HVDC coupling DC and provides the relevant statistics data in China.

In normal bipolar operation mode, as shown in Fig. 1a, the working current of HVDC system will almost flow between two DC transmission lines, such as #1 and #2 DC lines, and only very small direct current, whose influence on AC power grid can be neglected, will be injected into the earth.

In contrast, when the HVDC system works under MGC operation mode as shown in Fig. 1b, the working current will flow between #1 DC line and the earth. In this case, the huge direct current will be injected into the earth through the DC grounding electrode, which will result in obvious DC potential changes in a wide range of area, such as the DC potential difference between the grounding electrodes of #1 MT and #2 MT, whose connection types are all YN/yn0/d11, the actual situation of Jiangsu power grid.

As a result of aforementioned DC potential changes of the earth, a coupling DC will be excited in the circuit consisting of the earth, 500kV AC transmission line, MT's 500kV winding and its neutral-point ground-wire. This coupling DC will also flow through the primary winding of 500kV CT, and then cause the DC bias phenomenon in the iron core of CT.

According to statistic, the MGC operating condition totally happened 105 times in all HVDC systems of State Grid from 2006 to 2012. On average, every pole quitted operation 1.3 times, about 37.8 hours, per year. Therefore, the coupling DC problem due to MGC operating condition and its bias influence on CT have attracted more and more attentions [13].

### III. DIGITAL SIMULATION METHOD FOR CT UNDER DC BIAS

In this section, in order to reveal the action mechanism of coupling DC on CT, a digital simulation method, based on Preisach magnetization theory, is established, and then its correctness is verified by error calibration experiment.

#### A. MATHEMATICAL MODEL BASED ON PREISACH THEORY

Based on the WIPING-OUT characteristics of Preisach theory and variable separation method, Zhang established a novel magnetization model of CT's iron core which can

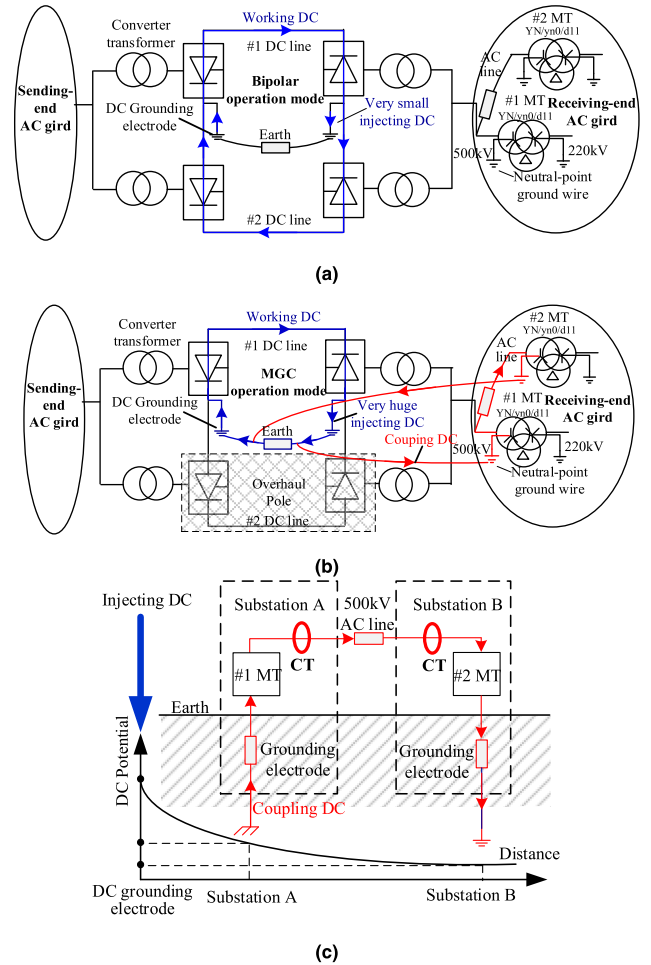


FIGURE 1. The generation mechanism of coupling DC. (a) Bipolar operation mode, (b) MGC operation mode and (c) The flowing path of coupling DC.

describes any hysteresis loop precisely [14], [15]. Firstly, the declining and ascending curves of limit hysteresis loop can be obtained through excitation experiments, and then any other magnetization curve can be calculated using (1) to (4).

$$F(H) = \begin{cases} \frac{B_d(H) - B_u(H)}{2\sqrt{B_d(H)}}, & H \geq 0 \\ \frac{B_d(-H)}{\sqrt{B_d(-H)}}, & H < 0 \end{cases} \quad (1)$$

where  $B$  represents magnetic flux density,  $H$  represents magnetic strength,  $B_d(H)$  and  $B_u(H)$  represent the declining and ascending curves of limit hysteresis loop, respectively.

$$B_{H_0, B_0}^u(H) = -B_d(-H) - B_d(H_0) + B_0 + 2F(-H_0) \cdot F(H), \quad H > H_0 \quad (2)$$

$$B_{H_0, B_0}^d(H) = B_d(H) + B_d(-H_0) + B_0 - 2F(H_0) \cdot F(-H), \quad H < H_0 \quad (3)$$

where  $B_{H_0, B_0}^d(H)$  and  $B_{H_0, B_0}^u(H)$  represent the declining and ascending curves starting from the extreme point  $(H_0, B_0)$ ,

respectively.

$$B_i(H) = \begin{cases} \left[ \frac{B_d(H) + B_u(H)}{2} \right]^2 \cdot [B_d(H)]^{-1}, & H \geq 0 \\ - \left[ \frac{B_d(-H) + B_u(-H)}{2} \right]^2 \cdot [B_d(-H)]^{-1}, & H < 0 \end{cases} \quad (4)$$

where  $B_i(H)$  represents the basic magnetization curve.

Substituting the total current equation

$$H \cdot l_m = N_1 \cdot i_1 - N_2 \cdot i_2 = N_2 \cdot i'_1 - N_2 \cdot i_2 = N_2 \cdot i_m \quad (5)$$

into the secondary electromagnetic induction equation of CT

$$N_2 \cdot A \cdot \frac{dB}{dt} = u_2 = i_2 \cdot R_2 + L_2 \cdot \frac{di_2}{dt}, \quad (6)$$

we can get a differential equation for solving the magnetic flux density  $B$  and exciting current  $i_m$ .

$$L_2 \cdot \{i_m[k] - i_m[k-1]\} \cdot F_s + N_2 \cdot A \cdot F_s \cdot \{B[k] - B[k-1]\} + i_m[k] \cdot R_2 = L_2 \cdot F_s \cdot \{i'_1[k] - i'_1[k-1]\} + i'_1[k] \cdot R_2 \quad (7)$$

where  $i_1$  and  $i_2$  are the primary and secondary current,  $N_1$  and  $N_2$  are the turns of primary and secondary coils,  $l_m$  and  $A$  are the length and area of magnetic path,  $u_2$  is the secondary voltage,  $R_2$  and  $L_2$  are the secondary leakage resistance and reactance,  $i'_1 = (N_1 \cdot i_1)/N_2$  is the equivalent primary current,  $F_s$  represents sample frequency, and  $k$  represents the serial number of discrete sampling.

## B. DIGITAL SIMULATION TOOL

The schematic diagram of proposed digital simulation tool is given in Fig. 2. It mainly consists of three modules:

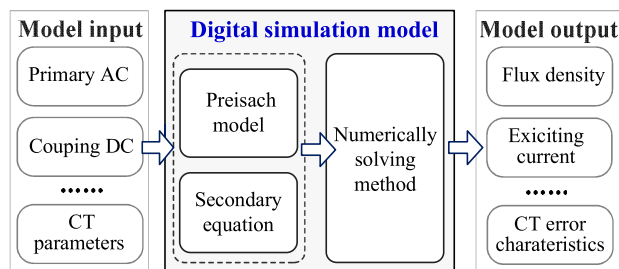


FIGURE 2. Schematic diagram of digital simulation tool.

### 1) PREISACH MAGNETIZATION MODEL

Using Preisach magnetization model, from (1) to (4), we can solving any magnetization curve when the iron core is unsaturated.

### 2) SECONDARY ELECTROMAGNETIC INDUCTION EQUATION

As there are total two unknowns  $B$  and  $i_m$  (or  $H = N_2 \cdot i_m/l_m$ ) in the equations of Preisach magnetization model and secondary electromagnetic induction, from (5) to (7), we can solve  $B$  and  $i_m$  by jointly solving them.

### 3) NUMERICALLY SOLVING METHOD FOR NON-LINEAR DIFFERENTIAL EQUATIONS

Due to the monotonic characteristic of magnetization curve, we can use the heuristic method to solve the non-linear differential equations consisting of magnetization curve and electromagnetic induction.

When simulating the working state under DC bias, the coupling DC, primary AC and CT's parameters, such as declining curve of limit hysteresis loop, iron core size, winding turns and secondary impedance, are input into this digital tool. After numerically solving, the whole transient magnetization process of iron core can be calculated and output, which means that the magnetic flux density, exciting current, secondary current and the error characteristics of CT can all be observed clearly. The digital simulation tool is self-developed by Zhou and Cai using VC++ and more details can be seen in [16].

## C. EXPERIMENT VALIDATION OF DIGITAL SIMULATION METHOD

In order to verify the correctness of proposed simulation method, an error calibration system, which can generate AC and DC hybrid large current in the same cable, is established. As shown in Fig. 3, due to the existence of blocking capacitance, only AC can circulate through the reference CT, while both AC and DC can flow into the tested CT. The second currents of aforementioned two CTs are input into the calibrator. Taking the reference CT as a benchmark, the ratio error of tested CT under different coupling DC level is calculated as follows.

$$\varepsilon_C = \frac{I_{2, \text{tested}} - I_{2, \text{ref}}}{I_{2, \text{ref}}} \times 100\% \quad (8)$$

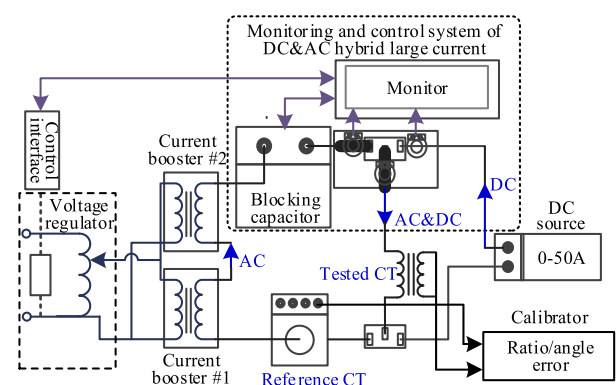


FIGURE 3. The error calibration system for CT in DC bias condition.

where  $I_{2, \text{ref}}$  and  $I_{2, \text{tested}}$  are the effective value of secondary fundamental current of reference CT and tested CT, respectively.

In contrast, the simulation result of ratio error is calculated as follows.

$$\varepsilon_S = \frac{I_2 - I'_1}{I'_1} \times 100\% \quad (9)$$

where  $I_1' = (N_1 \cdot I_1)/N_2$  is the effective value of equivalent primary fundamental current, and  $I_2$  is the simulation result of effective value of secondary fundamental current.

The correctness of simulation method can be verified by comparing its calculation results with experimental results of calibration system. Using the proposed simulation tool and calibration system respectively, the error characteristics of a 500kV measuring CT sample under different coupling DC have been analyzed and compared. The simulation parameters of tested CT sample are listed in Table 1. As shown in Fig. 4, the maximal relative error between the simulation and experiment is less than 3.5% when the coupling DC  $I_{dc}$  varies from 0A to 30A. It proved that our simulation method is accurate enough to study the action mechanism of DC bias.

TABLE 1. The simulation parameters of 500kV measuring CT Sample.

Parameter name	Value
Magnetic circuit size	205.37cm×3.25cm <sup>2</sup>
Turns ratio	2: 4000
Rated transformation ratio	2000/1 A
Rated second load	15VA and power factor $\lambda=0.8$
Second leakage impedance	13.5 + 0.1j $\Omega$ at 75°C
Core material	1k107 ultra-fine crystalline <sup>a</sup>

<sup>a</sup> Its declining branch of limit hysteresis loop was obtained by low-voltage measuring system mentioned in [17].

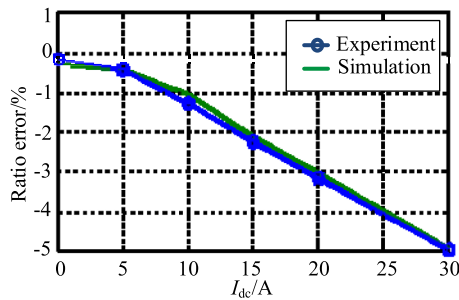


FIGURE 4. Comparison of ratio error between experiment and simulation.

#### IV. INFLUENCE MECHANISM OF COUPLING DC ON CT

In this section, using the digital simulation method proposed in Section III, the inherent mechanism of DC bias phenomenon will be analyzed.

We choose a 500kV measuring CT with the 1k107 ultra-fine crystalline core as analysis object, whose parameters are listed in Table 1, and the coupling relationships among the magnetic flux density  $B$ , exciting current  $I_m$  and coupling DC  $I_{dc}$  are simulated. The magnetic flux density under 0A and 20A coupling DC are given in Fig. 5. The peak value of flux density and exciting current varying with coupling DC are given in Fig. 6. The influence mechanism of coupling DC can be concluded as follows.

1) The 1k107 ultra-fine crystalline is one of common materials for iron core of measuring CT. The present design principle for measuring CT, regardless of the

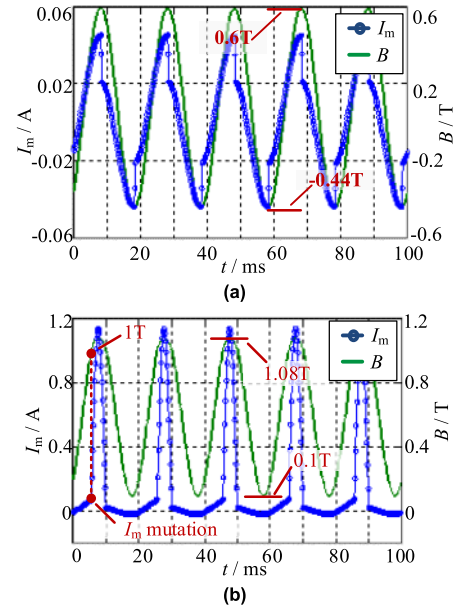


FIGURE 5. Simulation results of measuring CT under rated condition. (a) No coupling DC and (b) 20A coupling DC.

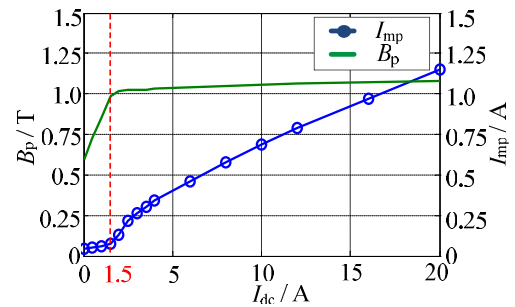


FIGURE 6. The relationship curves of  $B_p$  and  $I_{imp}$  varying with  $I_{dc}$ .

coupling DC, is making flux density operate in the middle of magnetization-curve linear region when CT is under rated condition. The saturate flux density of 1k107 material is about 1T. Correspondingly, as shown in Fig. 5a, it can be observed that the flux density  $B$  works approximately in the middle of linear region (from  $-0.44T$  to  $0.6T$ ), which is well consistent with aforementioned CT design principle. Under this condition, the saturate phenomenon of iron core never happens and thus the exciting current  $I_m$  is very small (about  $0.04A$ ). In addition, it can be observed that the stable waveform of  $B$  is a sine wave with a little positive deviation. The reason is that the primary current was imposed from 0A and varied towards positive direction, so there existed an electromagnetic transient process, which is recorded by the iron core and resulted in the slight asymmetry of magnetic flux  $B$ .

2) As shown in Fig. 5b, with the excitation of 20A positive coupling DC, the working area of iron core moved upward obviously and the magnetic flux  $B$  fluctuated



between 0.1T to 1.08T. Of particular note is that, when  $B$  exceeds 1T, the iron core begins saturate and the corresponding exciting current  $I_m$  will increase suddenly, from 0.1A to 1.15A.

- 3) As shown in Fig. 6, the curve slopes of peak value of flux density  $B_p$  and peak value of exciting current  $I_{mp}$  change greatly when the coupling DC  $I_{dc}$  arrives 1.5A, so correspondingly we divide the severity of DC bias into two different levels: slight condition  $I_{dc} < 1.5A$  and serious condition  $I_{dc} > 1.5A$ . When the iron core is under slight bias condition,  $B_p$  has not entered into the saturation region and so the increment of  $I_{mp}$ , with  $I_{dc}$  increasing, is very small, which means that the influence of slight bias on measuring accuracy can be neglected. In contrast, when the iron core is under serious bias condition,  $B_p$  has entered into the deep saturation region and so it will grow very slowly at the cost of dramatic increase of  $I_{mp}$ . Therefore, the serious bias condition will affect the transfer characteristics of CT greatly.
- 4) In addition, the effect of negative coupling DC is similar with that of positive coupling DC analyzed above and so not discussed here.

**V. INFLUENCE ASSESSMENT OF HVDC TRANSMISSION SYSTEM ON CT'S MEASURING ACCURACY**

In this section, the measured data of coupling DC and its influence on CT's measuring accuracy are analyzed.

The  $\pm 800$  kV Tongli converter station of J2SJ HVDC system is taken as a research object. The rated transmission capacity of J2SJ HVDC system is 7, 200MW which can meet the summer power supply of Nanjing city, Jiangsu Province. In order to measure the actual coupling DC, within 100km radius of the grounding electrode of Tongli converter station, totally 23 DC detecting devices have been installed on the neutral points of MTs. Thus, as shown in Fig. 7, a coupling DC monitoring network has been established.

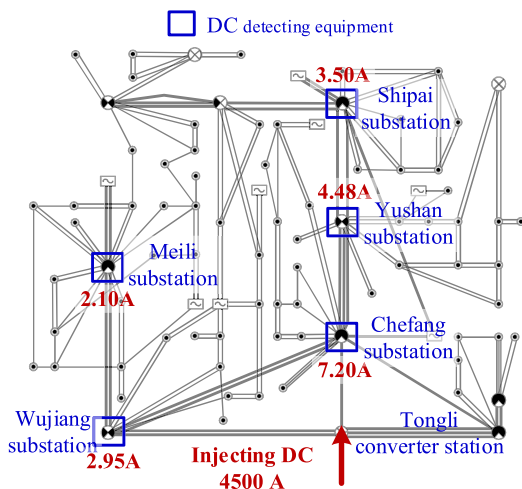


**FIGURE 7. The monitoring network of Coupling DC for J2SJ HVDC system.**

During July 6th to 8th 2012, the J2SJ HVDC system was under the MGC operation mode and there was about 4500A working DC injected into the earth through Tongli grounding electrode. At that time, our monitoring system detected the comparatively large coupling DC in the nearby AC power grid. Table 2 lists ten MTs affected most seriously. The average value of coupling DC was about 3.63A and the maximal coupling DC, about 7.20A, occurred in #2 MT in Chefang substation. Assuming that the coupling DC through neutral point of MT will flow into three-phase lines on average, there was about 2.40A ( $2.40 = 7.20/3$ ) coupling DC acting on line CT.

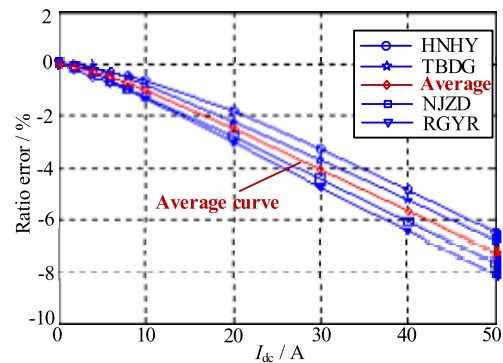


**FIGURE 8. Ratio error characteristics varying with coupling DC.**

**TABLE 2. Monitoring data of coupling DC and corresponding CT error.**

Main transformer	Coupling DC (A)	CT error (%)
Wujiang substation #1	2.80	-0.0165
Wujiang substation #3	2.95	-0.0197
Yushan substation #1	4.48	-0.0541
Yushan substation #4	4.34	-0.0513
Chefang substation #2	7.20	-0.1234
Chefang substation #3	3.80	-0.0389
Shipai substation #2	3.50	-0.0321
Shipai substation #3	3.20	-0.0255
Meili substation #1	2.10	-0.0023
Meili substation #2	1.95	-0.0007

In order to evaluate the influence of coupling DC on actual CTs in power grid, we firstly investigated the CTs used in aforementioned ten MTs. There are totally four types of CT from the following manufacturers: HNHY, TBDG, NJZD and RGYR. Then, as shown in Fig. 8, the error characteristics of these CTs, varying with coupling DC, are measured by the error calibration system mentioned in section III. Finally, by matching the average error curve in Fig. 8 and the coupling DC data listed in Table 2, the influence of coupling DC on CT's measuring accuracy can be evaluated quantitatively. For example, the ratio error of CT located in #2 MT of Chefang substation, which suffered about 2.40A coupling DC, has deviated negatively 0.123%, equivalent to 61.5% error limit value for 0.2S measuring CT.

With the rapid development of HVDC transmission projects, there will appear more and more multi-HVDC

receiving and sending ends in China, such as Jiangsu Province and Guangdong Province, where the phenomenon of coupling DC maybe becomes more serious. As shown in Fig. 8, when the neutral point DC reaches 9.45A (3.15A on line CT), the deviation of ratio error will exceed 0.2%, the error limit value of 0.2S measuring CT. Therefore, how to resist the negative influence of HVDC system on measuring CT has become an urgent problem.

## VI. CONCLUSION

This paper focuses on analyzing the bias influence of HVDC coupling DC on CT. Our main contributions include:

- 1) Based on Preisach magnetization theory, a digital simulation method for CT is proposed and used to analyze the inherent mechanism of DC bias phenomenon. The comparison with calibration experiments shows that this simulation method is accurate enough to be a convenient and fast substitute for experimental method.
- 2) Our most important contribution is that a coupling-DC monitoring network for J2SJ HVDC system is built, and then based on the measured data and analysis results of CT's error varying with coupling DC, the actual influence of J2SJ HVDC system on nearby CTs is evaluated. It is found that when the coupling DC through MT neutral-point reaches 9.45A, the deviation of ratio error will exceed 0.2% (the error limit value of 0.2S measuring CT).

In China, there will appear more and more multi-HVDC receiving and sending ends, where the problem of coupling DC maybe becomes more serious. Our further studies involve how to resist the increasingly severe influence of coupling DC on CT.

## REFERENCES

- [1] N. Florentzou, V. G. Agelidis, and G. D. Demetriades, "VSC-based HVDC power transmission systems: An overview," *IEEE Trans. Power Electron.*, vol. 24, no. 3, pp. 592–602, Mar. 2009.
- [2] M. P. Bahrman and B. K. Johnson, "The ABCs of HVDC transmission technologies," *IEEE Power Energy Mag.*, vol. 5, no. 2, pp. 32–44, Mar. 2007.
- [3] W. Lu and B. Ooi, "Optimal acquisition and aggregation of offshore wind power by multiterminal voltage-source HVDC," *IEEE Trans. Power Del.*, vol. 18, no. 1, pp. 201–206, Jan. 2013.
- [4] W. Li, Z. Pan, H. Lu, X. Chen, L. Zhang, and X. Wen, "Influence of deep Earth resistivity on HVDC ground-return currents distribution," *IEEE Trans. Power Del.*, vol. 32, no. 4, pp. 1844–1851, Aug. 2017.
- [5] R. Zeng, Z. Yu, J. He, B. Zhang, and B. Niu, "Study on restraining DC neutral current of transformer during HVDC monopolar operation," *IEEE Trans. Power Del.*, vol. 26, no. 4, pp. 2785–2791, Oct. 2011.
- [6] D. C. Yu, J. C. Cummins, Z. Wang, H.-J. Yoon, and L. A. Kojovic, "Correction of current transformer distorted secondary currents due to saturation using artificial neural networks," *IEEE Trans. Power Del.*, vol. 16, no. 2, pp. 189–194, Apr. 2001.
- [7] S. Lu, Y. Liu, and J. De La Ree, "Harmonics generated from a DC biased transformer," *IEEE Trans. Power Del.*, vol. 8, no. 2, pp. 725–731, Apr. 1993.
- [8] F. Yang, F. Dai, X. Liu, Y. Yang, and W. He, "Investigation on the magnetic bias current and electromagnetic force of power transformer in multi-layer soil area," *Int. J. Appl. Electromagn. Mech.*, vol. 47, no. 8, pp. 791–804, 2015.
- [9] P. Ripka, K. Draxler, and R. Stybliková, "DC-compensated current transformer," *Sensors*, vol. 16, no. 1, pp. 212–215, 2016.
- [10] C.-Y. Li, Q.-M. Li, Z. Li, and Q.-Q. Sun, "Transfer characteristics of current transformers with DC bias," *Proc. CSEE*, vol. 30, no. 19, pp. 127–132, 2010.
- [11] U. D. Annakkage, P. G. McLaren, E. Dirks, R. P. Jayasinghe, and A. D. Parker, "A current transformer model based on the Jiles-Atherton theory of ferromagnetic hysteresis," *IEEE Trans. Power Del.*, vol. 15, no. 1, pp. 57–61, Jan. 2000.
- [12] S. Yang, Z. Wei, J. Cai, G. Zhou, and Z. Wang, "Research on the influence of HVDC transmission on measuring accuracy of current transformers," in *Proc. IEEE Int. Magn. Conf. (INTERMAG)*, May 2015, p. 1.
- [13] Z. Liang, Y. Dong, and Z. Zhang, "Statistical analysis on forced outages of HVDC transmission systems in state grid corporation of China from 2006 to 2012," *Autom. Electr. Power Syst.*, vol. 38, no. 6, pp. 1–5, 2014.
- [14] A. Rezaei-Zare, R. Iravani, M. Sanaye-Pasand, H. Mohseni, and S. Farhangi, "An accurate current transformer model based on Preisach theory for the analysis of electromagnetic transients," *IEEE Trans. Power Del.*, vol. 23, no. 1, pp. 233–242, Jan. 2008.
- [15] X.-G. Zhang and Z.-Z. Wang, "Research on CT modeling based on the Preisach theory," *Proc. CSEE*, vol. 25, no. 8, pp. 68–72, 2005.
- [16] S. Lu, S. Yang, J. Cai, G. Zhou, and M. Xu, "Action principle of DC magnetic bias to current transformer," *Electr. Meas. Instrum.*, vol. 51, no. 14, pp. 6–11, 2014.
- [17] H.-Z. Cui et al., "Low-voltage measuring system for limiting magnetic hysteresis loop of iron core," *Electr. Meas. Instrum.*, vol. 50, no. 7, pp. 53–57, 2013.



**SHIHAI YANG** received the B.S. degree in electrical engineering from the Hefei University of Technology, Hefei, China, in 1999, and the M.S. degree in electrical engineering from Southeast University, Nanjing, China, in 2004. He is currently pursuing the Ph.D. degree with Hohai University. He is currently with the Electric Power Research Institute, Jiangsu Electric Power Company. His current research interests include electric energy metering and smart power utilization.



**GAN ZHOU** (M'09) received the M.S. and Ph.D. degrees from the School of Electrical Engineering, Southeast University, Nanjing, China, in 2003 and 2009, respectively. He is currently an Associate Professor with the School of Electrical Engineering, Southeast University. His current research interests include electric energy metering and high-performance computing in power system.



**ZHINONG WEI** received the B.S. degree from the Hefei University of Technology, Hefei, China, in 1984, the M.S. degree from Southeast University, Nanjing, China, in 1987, and the Ph.D. degree from Hohai University, Nanjing, in 2004. He is currently a Professor of electrical engineering with the College of Energy and Electrical Engineering, Hohai University. His research interests include power system state estimation, integrated energy systems, smart distribution systems, optimization and planning, load forecasting, and integration of distributed generation into electric power systems.